BEAM-COLUMN JOINT BEHAVIOR AFTER BEAM YIELDING IN R/C DUCTILE FRAMES

Osamu JOH[1] And Yasuaki GOTO[2]

SUMMARY

Ductile behavior of reinforced concrete frame during severe earthquake is obtained by large energy dissipation in yield hinge formed at beam end without beam-column joint failure. Joint failure occurs due to large shear input from beam, bond deterioration of beam bars by cyclic loading and lack of confinement for joint core concrete. In this study, the effect of joint failure after beam yielding on frame behavior is examined based on the two experimental studies of plane beam-column sub-assemblages and tree-dimensional ones. In plane frame test, to examine the effect of joint shear input and beam bar condition on frame behavior, six half-size specimens were tested, which had differences in beam bar area (2 variations) and bar diameter (3 variations). In 3-dimensional frame test, to examine the effect of transverse beams and loading history on joint performance, four half size specimens were tested which had difference in joint input (beam bar area: 2 variations) and bond condition (diameter: 2 variations) and also had slabs. Following conclusions are derived from two experimental studies: 1) Beam bar condition in joint did not make a large influence on energy dissipation of frame, if joint shear failure occurred after beam yielding. 2) Joint shear strength was increased by the existence of transverse beams. 3) The damage of joint core concrete in one way loading made weak in frame performance in perpendicular loading.

INTRODUCTION

Reinforced Concrete Earthquake Resistant Frame is designed on the basis of "strong-column weak-beam" concept. Generally ductile frame behavior would be ensured by energy dissipation which is expected in the yield hinging at beam end. Whereas the frame was designed to be failed in beam flexural, shear failure in beam-column joint occurred after beam yielding at large displacement in 1995 Hyogo-ken Nanbu earthquake. Recently a number of researches on RC beam-column joint were carried out and then some estimation formula for joint shear strength was proposed. But in some experimental study, joint shear failure occurred at large displacement, even the joint shear strength was sufficient larger than beam flexural strength. So the reason why the joint shear failure occurs after beam yielding, even though the frame is designed ductile, should be clarified immediately, and also the influence on frame performance should be understood. In this study, the effect of joint shear input at beam yielding and beam bar bond condition within joint on frame behavior after beam yielding were examined experimentally.

EXPERIMENTAL WORK

Plane Flame Test
Specimens
Six specimens of interior beam-column assemblages were the same shape and size; cross shaped, half size of actual, column of 300mm x 300mm, beam of 200mm x 350mm, column height of 1750mm, beam span of 3000mm, and without slabs nor transverse beams. To make sure that beam yielding occurs prior to other failure, beam flexural strength was designed smaller than shear strength of beam, column and joint. Specimen parameters are 2 levels of joint shear input (beam bar area) and 3 types of bond condition (beam bar diameter).

[1] *Architectural Engineering, Graduate School of Engineering, Hokkaido University, Sapporo Japan*
[2] *Architectural Engineering, Graduate School of Engineering, Japan Email: gottsu@eng.hokudai.ac.jp*

Specimen name is consisted of 2 capital letters and number which represent joint input level (High or Low) and bar diameter (10, 13 and 16), respectively. Reinforcement detail is shown in Fig.1 and Table 1.
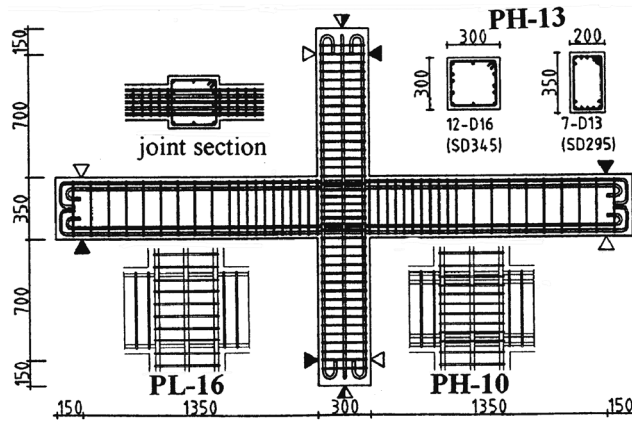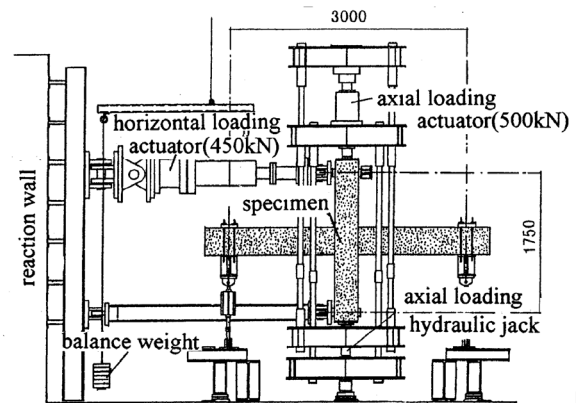

Fig. 1   Specimen (Plane Frame)

Fig. 2   Loading Arrangement

Table 1   Properties of Specimens (Plane Frame)

specimen	beam bar [Double layered]	D_c/d_b	$a_t \cdot \sigma_y$ (kN)	joint shear input $v_j / \sqrt{\sigma_B}$	column bar	joint
PL-16	3-D16	18.8	204	0.865	10-D16	ϕ-6
PL-13	5-D13	23.1	213	0.912	SD345	6 sets
PL-10	8-D10 [4/4]	30.0	199	0.803	p_g=2.21%	0.37%
PH-16	4-D16	18.8	272	1.232	12-D16	ϕ-6
PH-13	7-D13 [5/2]	23.1	298	1.248	SD345	8 sets
PH-10	10-D10 [5/5]	30.0	249	1.095	p_g=2.65%	0.47%

Dc:column depth d_b:beam bar diameter

Table 2   Properties of Materials

Concrete	σ_B (MPa)	ε_{max} (μ)	σ_t (MPa)	E_c (GPa)	Steel	σ_y (MPa)	ε_y (μ)	σ_u (MPa)	elong. (%)	E_s (GPa)
PL-16	26.9	2620	2.24	26.7	$\phi 6$	366	1950	437	18.5	197
PL-13	26.4	2730	2.46	22.2	D10	372	2010	525	19.4	195
PL-10	30.4	2740	2.37	23.7	D13	363	1930	517	20.9	198
PH-16	23.6	2660	1.98	20.9	D16beam	344	2100	491	24.2	172
PH-13	26.3	2920	2.48	20.8	D16column	402	2280	575	27.4	185
PH-10	25.6	2710	2.28	21.0						

Concrete compressive strength (σ_B) was 20 MPa, and reinforcement were SD295 of beam bars, SD345 of column bars and SR295 of transverse reinforcement. Material properties are shown in Table 2.
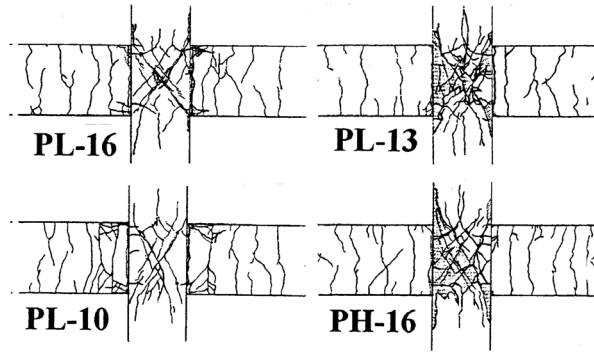
Low input specimens: Joint shear stress at beam yielding is designed square root of concrete compressive strength, in which slight shear crack would be observed due to such joint input. Top and bottom beam bar arrangements were 3-D16, 5-D13 (single layered) and 8-D10 (double layered), which were almost the same in area. Joint reinforcement ratio is 0.37%.

High input specimens: Joint shear stress at beam yielding is designed 1.4 times of square root of concrete compressive strength, in which shear deterioration of joint concrete would be observed after beam yielding at large displacement. Top and bottom beam bar arrangements were 4-D16 (single layered) and 7-D13, 10-D10 (double layered), which were almost the same in area. Joint reinforcement ratio is 0.47%.
Heavy reinforcement is provided at beam ends, not to occur bond deterioration of beam bars in this region.

Loading and Instrumentation
Loading arrangement is schematically shown in Fig. 2. The incremental forced displacement was given to the specimen at top of column cyclically during column axial stress of $\sigma_B/6$ had been applied. The forces, displacement and reinforcement strains were measured during test.

shade : spalling of concrete
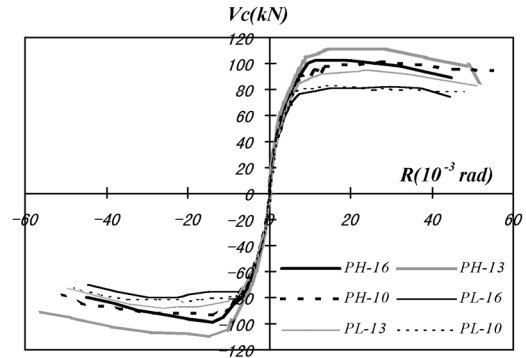
Fig. 3 Crack Pattern after Test

Fig. 4 Column Shear vs. Story Drift Angle

Specimen Behavior

Crack pattern of each specimen after test is shown in Fig. 3, and envelope curves of column shear (Vc) vs. story draft angle (R) relationship are shown in Fig. 4.

Low input specimens : Flexural cracks at beam ends extended obviously and joint shear cracking was fractional, finally whole beam bars were yielded in all specimens. But joint concrete crashing observed at the large displacement inPL-13, which is slightly larger in joint input than other specimen. In this specimen crack width of beam flexural and joint shear were almost equal at the 4 times displacement of yielding, but large concrete spalling in joint was observed. Strength decay is not observed in the specimens failed in beam flexural but in PL-13 over $R=20 \times 10^{-3}$rad

High input specimens : Beam yielding was observed in all specimens. After that, joint shear crack expanded widely and concrete spalling in joint was obviously at the large displacement loading cycle. Ultimate strength was gained at story drift angle of between 20 to 30×10^{-3}rad in each specimen, and then strength decay appeared. A few of joint reinforcement in the middle of joint were yielded at ultimate stage.

Strength

Test results of cracking, yielding and ultimate strength and the comparison with the calculated values were shown in Table 3.

Joint shear cracking strength ware larger than the calculated value of the principal stress equation and this tendency was remarkable in the specimen of thin beam bar. Ultimate strength was lager than the calculated value by 20% in low input specimens, but only less than 10% in high input specimen except to PH-10. The ratio of joint shear stress at ultimate strength to designed joint shear strength of $1.7\sqrt{\sigma_B}$ (MPa) is between 0.56 to 0.7 in low input specimens, and between 0.72 to 0.83 in high input specimens.

Equivalent viscous dumping factor

Equivalent viscous dumping factor (heq) calculated from column shear - story drift hysteresis loop is shown in Fig. 5. It reached maximum at the ultimate strength and the values at 2nd loading of $R=20 \times 10^{-3}$rad were still more than 0.1, which is the criterion of bond behavior proposed in AIJ guideline based on the ultimate strength. In particular PL-10 showed good performance in energy dissipation, but the value of PL-16 was almost the same as PL-13 whereas joint shear deterioration was slight. It is thought that bond deterioration of beam bars in joint was remarkable in PL-16. In high input specimen, there is no difference in the values, which shows no influence of bond condition on the energy dissipation on condition that joint shear deterioration was occurred.

2.1.6 Deflection components of story drift

The contribution of beam rotation and joint shear distortion to story drift is shown in Fig. 6. Beam rotation is calculated from slip (pull-out and push-in) of top and bottom bars at beam end. In case of double layered, the values of outer bars were available. Beam rotation component became large after the ultimate in PL-10 and PL-16, which were failed in beam flexural. Also it increased till the ultimate in PL-13, but then decreased whereas

Table 3   Test Result

Specimen		beam cracking Vc			joint cracking v_j			beam yielding Vc			ultimate Vc			failure mode
		exp	cal1	e/c	exp.	cal2	e/c	exp	cal3	e/c	exp	cal4	e/c	exp.Vj	
PL-16	+	24.7	18.1	1.37	3.52	3.05	1.15	76.6	68.9	1.11	82.0	70.9	1.16	5.16	B
	-	16.0		0.89	3.39		1.11	75.1		1.09	79.6		1.12	5.00	
PL-13	+	20.7	19.3	1.07	3.55	2.99	1.19	84.9	75.0	1.13	95.4	77.1	1.24	5.99	BJ
	-	17.0		0.88	3.13		1.05	82.2		1.10	87.8		1.14	5.52	
PL-10	+	27.1	19.1	1.42	4.34	3.28	1.32	79.3	66.2	1.20	83.7	68.1	1.23	5.64	B
	-	28.1		1.47	4.15		1.27	79.0		1.19	83.5		1.23	5.63	
PH-16	+	19.7	18.9	1.04	3.67	2.78	1.32	102.2	91.9	1.11	102.2	94.1	1.08	6.42	BJ
	-	17.9		0.95	3.16		1.14	98.6		1.07	98.6		1.04	6.20	
PH-13	+	12.6	20.5	0.62	4.02	2.98	1.35	104.1	101.2	1.03	111.0	104.6	1.06	7.25	BJ
	-	10.6		0.52	3.79		1.27	104.2		1.03	110.3		1.05	7.21	
PH-10	+	17.9	18.7	0.96	4.15	2.93	1.42	93.8	82.8	1.13	101.5	85.1	1.19	6.83	BJ
	-	10.5		0.56	3.60		1.23	88.4		1.07	92.3		1.08	6.22	

column shear : $V_c = \dfrac{2_b M}{l_{be}} \cdot \dfrac{l_b}{h_c}$ (kN)   joint shear stress : $v_j = \dfrac{(h_c \cdot l_{be} - l_b \cdot j_b)}{l_b \cdot j_b \cdot D_c \cdot t_p} \cdot V_c$ (MPa)

cal1: $_b M_{bc} = F_t \cdot Z_e$ $F_t = \beta \sqrt{\sigma_B}$ $\beta = 0.563$ cal2: $v_{cr} = \sqrt{F_t{}^2 + F_t \cdot \sigma_0}$ $F_t = \beta \sqrt{\sigma_B}$ $\beta = 0.438$

cal3: $_b M_{by} = a_t \cdot \sigma_y \cdot j_b$ cal4: $_b M_{bu} = 0.9 \cdot a_t \cdot \sigma_y \cdot d$

   l_b :beam span(mm) l_{be} :clear span(mm) h_c :column height (mm) D_c: column depth(mm) j_b :lever arm of beam=$7d/8$
   d:effective depth(mm) t_p:joint effective width(mm) a_t :beam bar area (mm^2) σ_0:column axial stress(MPa)
   Failure Mode B :beam flexural   BJ :joint shear failure after beam yielding

joint shear component increased.   Joint shear component increased remarkably in high input specimens, simultaneously beam rotation component was constant.

Bond stress distribution of beam bar

Bond stress distribution of top beam bars in PL-16, PH-13and PH-10 are shown in Fig. 7.   Bond stress was calculated from bar stress obtained by measured strain using Ramberg-Osgood model. The peak of distribution was located in the middle of joint at initial loading, but it moved column compressive zone after beam yielding in PH-10 and PH-13, which were failed in joint shear after beam yielding. This is because that concrete deterioration due to shear cracking occurred at the middle of joint. In other hands, the penetration of yield zone into joint generated large bond stress in the middle of joint in the specimen failed in beam flexural.
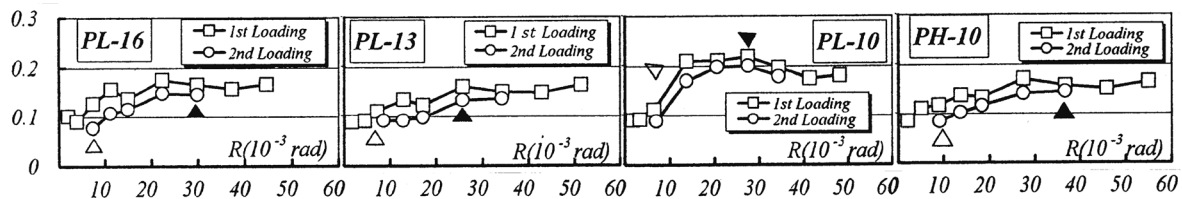

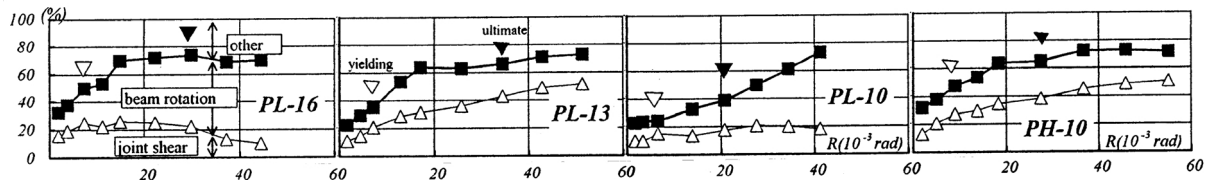
Fig. 5   Equivalent Viscous Dumping Factor

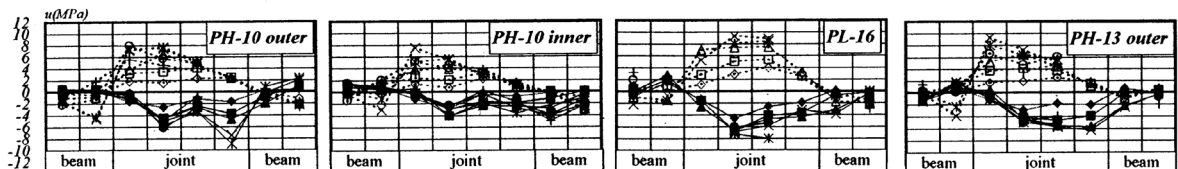**Fig. 6   Deflection Component of Story Drift**

Fig. 7   Bond Stress Distribution

Fig. 8 Specimen (Three-dimensional Frame)

Table 4 Properties of Specimen

	TH-13	TH-13A	TH-19	TL-13
parameter	basic	loading	bar diameter	joint input
column bar	16-D16(SD345) p_g=3.54%			12-D16 p_g=2.65%
beam bar (X,Y)	8-D13(SD295)[4/4] p_t=1.70%		3-D19(SD345) p_t=1.37%	5-D19(SD295) p_t=0.99%
$a_t \cdot f_y$	344(kN)		331(kN)	215(kN)
D_c/f_c	23.1		15.8	23.1

Table 5 Properties of Materials

Concrete	f_c (MPa)	ε_{max} (f_c)	f_t (MPa)	E_c (GPa)	Steel	f_y (MPa)	ε_y (f_y)	f_u (MPa)	elong. (%)	E_s (GPa)
TH-13	22.8	2840	1.99	22.8	D13	334	1920	477	29.0	191
TH-13A	19.7	2560	1.77	22.0	D19	384	2430	585	20.4	175
TH-19	20.3	2500	1.86	21.9	D16	387	2210	545	25.5	192
TL-13	23.2	2640	1.83	22.6	6φ hoop	373	2280	448	23.3	191
					6φ slab	291	3330	482	30.6	221

Tree Dimensional Frame Test

Specimens

Four specimens of interior beam-column assemblages were half size of actual and had transverse beams and slab. Dimensions of column and beams are the same as the plane frame specimen and slab thickness was 60mm which had single wire mesh (@200) of 6mm round bar. Each specimen was designed that beam flexural failure occurs prior to other failure and had difference in joint shear input at beam yielding and bond condition of beam bars. Joint shear input levels were 2 grade of $1.6\sqrt{\sigma_B}$ (High) and $1.1\sqrt{\sigma_B}$ (Low) in joint shear stress, which depended on beam bar strength and area. Bond condition was changed by bar diameter at 2 types of D13 and D19. Specimen name is consisted of 2 capital letters and number which represent joint shear input level (High or Low) and bar diameter (13 or 19), respectively. Also one specimen has the capital "A" in its name, which means the difference in loading rule. Reinforcement detail is shown in Fig. 8 and Table 4.

Concrete compressive strength (σ_B) was 20MPa, and reinforcement were SD295 of D13 (beam), SD345 of D19 (beam), D16 (column) and SR295 of slab bars. Material properties are shown in Table 5.

Low input specimen: Both top and bottom beam bar arrangement of specimen (TL-13) were 5-D13(single layered). Amount of joint reinforcement was 0.39%.

High input specimens: Beam bar arrangements were 3-D19(single layered) in specimen (TH-19) and 8-D13 (double layered) in two specimens (TH-13 and TH-13A). Amount of joint reinforcement was 0.77%.

Loading and Instrumentation

Loading arrangement was similar to that of plane frame test, but also there was another set in perpendicular way. All specimens were loaded cyclically with gradually increment in displacement. Three specimens were loaded one way and perpendicular alternately in the same displacement, but one specimen (TH-13A) was loaded only one way till ultimate stage and then perpendicular. The forces, displacement and reinforcement strains were measured during test.

Table 6   Test Result

Specimen	direc.	joint shear cracking					beam yielding					ultimate					
		expVj		cal2	exp/cal		expVc		cal3	exp/cal		expVc		cal4	exp/cal		effective width (mm)
		+	•		+	•	+	•		+	•	+	•		+	•	
TH-13	X	3.11	4.31	3.51	0.89	1.23	118	122	104	1.13	1.18	127	126	129	0.98	0.97	1200
	Y	3.92	3.57	3.51	1.12	1.02	113	102	114	0.99	0.89	116	108	130	0.90	0.83	1200
TH-13A	X	4.74	2.19	3.19	1.49	0.69	113	123	104	1.09	1.19	132	128	129	1.02	0.99	1200
	Y	2.65	2.94	3.19	0.83	0.92	99	101	114	0.87	0.89	103	101	130	0.79	0.78	1200
TH-19	X	5.92	3.50	3.25	1.82	1.08	122	119	106	1.15	1.13	126	123	137	0.92	0.90	1600
	Y	2.41	3.41	3.25	0.74	1.05	105	108	116	0.91	0.93	108	108	133	0.82	0.82	1200
TL-13	X	4.45	4.17	3.55	1.25	1.17	95.4	94.6	69.5	1.37	1.36	98.1	96.1	92.5	1.06	1.04	1200
	Y	3.35	3.23	3.55	0.94	0.91	83.0	82.5	75.9	1.09	1.09	86.1	85.4	93.4	0.92	0.91	1200

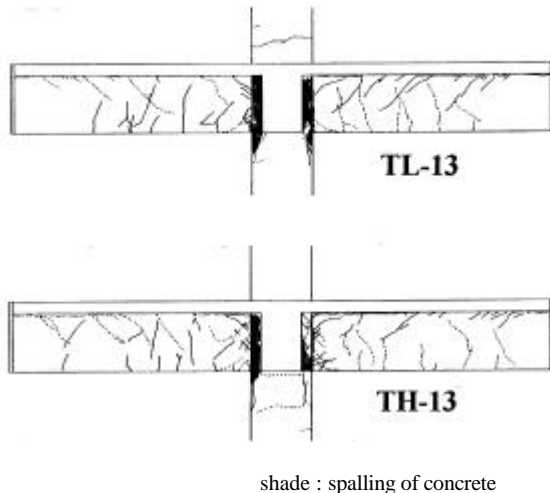Equations are shown in Table 3.

shade : spalling of concrete
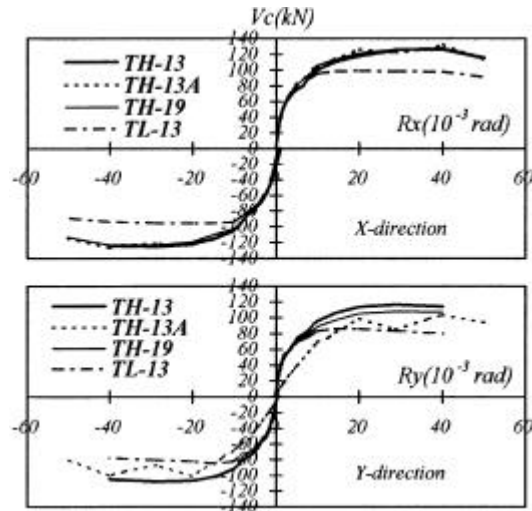**Fig. 9 Crack Pattern after Test (X-direction)**

Fig. 10   Column Shear vs. Story Drift Angle

Specimen behavior

Crack pattern of each specimen after test is shown in Fig. 9, and envelope curves of column shear (Vc) vs. story draft angle (R) relationship are shown in Fig. 10. Flexural cracking at beam ends occurred at R=1/500 loading cycle and joint shear cracking at R=1/200 in every specimen.

High input specimens (TH): Yield point in envelope curves is obscure, but half of beam bars were yielded at critical section till R=1/50, and then all were yielded finally. After R=1/35 loading cycle, joint shear cracks extended and spalling of joint corner concrete occurred at R=1/25 loading cycle. Strength decay on envelope curves was not obvious. Remarkable deterioration of stiffness and strength was observed in the Y-direction loading of TH-13A, because of the existence of severe damage on joint core concrete that occurred in prior X-direction loading up to the large displacement.

Low input specimen (TL): Yield point in envelope curve is obvious at R=1/100, when more than half of beam bars yielded. Flexural cracks at beam critical section extended till R=1/50 loading cycle, but then shear cracking in joint became remarkable and the spalling of joint corner concrete occurred.

Strength

Test results of cracking, yielding and ultimate strength and the comparison with the calculated values were shown in Table 5. Beam yielding strength in the X-direction loading was larger than that of Y-direction in each specimen, especially in TH-13A. Calculated flexural strength is considered with slab bars within the effective width of twice of beam width, based on AIJ RC standard. Assuming that the ultimate strength in experiment was limited by beam flexural failure, the effective slab width calculated from strain distribution were indicated in Table 5. They are the same in all specimens except for X-direction loading of TH-19, but the calculated strength considering these estimated effective width are larger than experimental value in Y-direction.

Equivalent viscous dumping factor

Equivalent viscous dumping factor (heq) calculated from column shear - story drift hysteresis loop in the X-direction loading is shown in Fig. 11. The minimum value was gained at R=1/70 in every specimen, when hysteresis loop changed from spindle-shape into reverse-S shape due to bond deterioration of beam bars within joint and remarkable shear cracking in joint. The value at 2nd loading of R=1/50 was smaller than 0.1 even in the
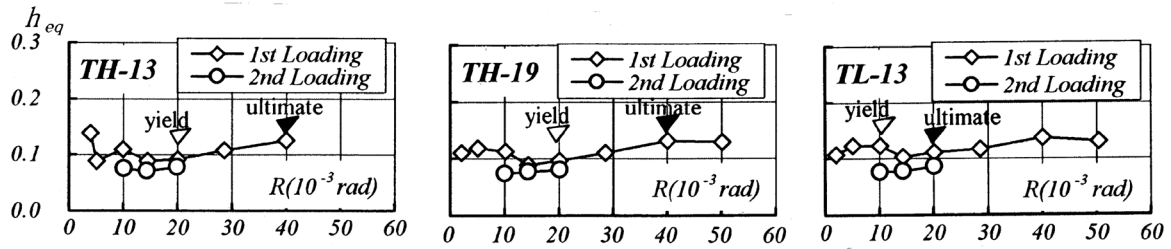
Fig. 11   Equivalent Viscous Dumping Factor (X-direction)

low input specimen.

Deflection components of story drift

The contribution of beam rotation and joint shear distortion to story drift in the X-direction loading is shown in Fig. 12. Joint shear component had been larger than beam rotation from beam yielding in high input specimen, while beam rotation component kept constant. Beam rotation component had been larger than joint shear component till the ultimate strength in TL-13, but then this inequality was reserved, obviously in backward loading.

Bond stress distribution of beam bars

Bond stress distributions of top beam bar in the X-direction loading of TL-13 and TH-13 are shown in Fig. 13. The peak of distribution in outer bar of TH-13 moved to column compressive zone after R=1/100 loading, while bond stress in joint kept constantly almost zero in inner bar. This is because that inner beam bars behaved as joint reinforcement, so that tensile stress was generated at whole region in joint due to shear cracking. The peak of distribution moved to column compressive zone even in TL-13 failed in beam flexural.
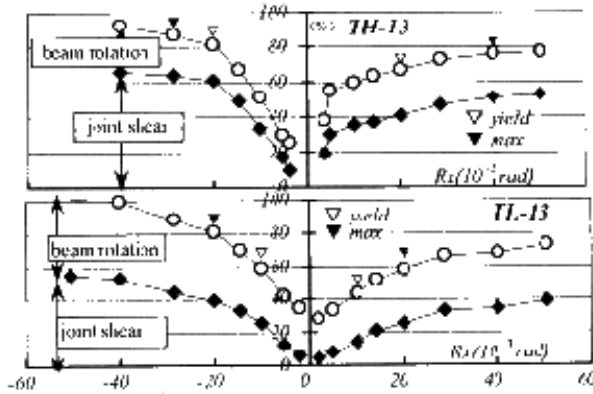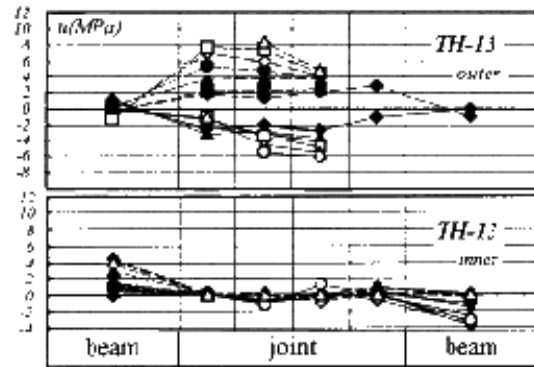

Fig. 12   Deflection Component of Story Drift

Fig. 13   Bond Stress Distribution

DISSCUSSION

Comparison between Plane Frame Test and Three Dimensional Frame Test

Strength

The comparison of the ultimate strength with the calculated value from the equation (1) proposed at AIJ guideline based on inelastic displacement concept are shown in Table 6.

$$V_{ju} = \kappa \phi F_j b_j D_j \qquad (1)$$

where, κ : factor of joint shape, 1.0 if cross shaped

   ϕ : factor of transverse beams,   1.0 if exist in both sides, 0.85 in other case

   F_j : fundamental shear strength, $= 0.8\sigma_B^{0.7}$ (MPa)

   b_j : joint effective width

   D_j : column depth

TABLE 7   JOINT SHEAR STRENGTH

Specimens	σ_B (MPa)	expVj (MPa) +	-	cal eq.(1)	exp/cal +	-
PL-13	26.4	5.99	5.52	6.72	0.89	0.82
PH13	26.3	7.25	7.21	6.71	1.08	1.07
TH-13 (X)	22.8	8.42	8.32	7.31	1.18	1.14
(Y)		8.54	7.96		1.17	1.09
TH-13A(X)	19.7	8.76	8.49	6.44	1.36	1.32
(Y)		7.57	7.41		1.18	1.15
TL-13 (X)	23.2	6.05	5.92	7.23	0.84	0.82
(Y)		5.81	5.76		0.80	0.80

The ultimate strength of low input specimens were less than the calculated by 10 or 20% in both test series, that of high input specimens were lager by 10% in plane frame and 20% in three dimensional frame. As beam yielding occurred in all specimens, the ultimate strength must be limited by beam flexural even in the high input specimen. The equation makes underestimation in joint shear strength.

Energy dissipation

In plane frame test, equivalent viscous dumping factor (*heq*) of the specimen failed in beam flexural was still more than 0.1 at 2nd loading in R=1/50. Low input specimen performed well at energy dissipation. Three-
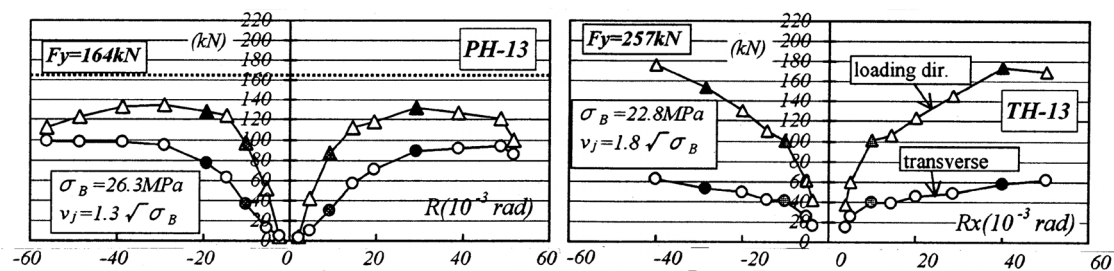

Fig. 14   Forces acting in Joint Reinforcement

dimensional frame test showed inferior behavior in energy dissipation even in the specimen failed in beam flexural. It is considered that the perpendicular loading made damage in joint concrete and bad influence on bond condition. But *heq* value kept less than 0.1 at 2nd loading in R=1/50 also in the X-direction loading of TH-13A, in which it was not loaded perpendicularly before. It is suspected that beam bars congested in joint made weak in bond condition.

Joint reinforcement and transverse beams

Sum of force acting in joint reinforcement located between top and bottom beam bars in loading direction and perpendicular are shown in Fig. 14. Forces acting in loading direction and perpendicular are considered as shear resistance and confinement of joint core concrete, respectively.

The ratio of forces acting in perpendicular to that in loading direction at the ultimate were more than 60% in the PH-13, but almost 30% in the three dimensional specimens. This means that transverse beams contributed to the confinement of joint concrete even after yielding.

Joint Shear Deterioration after Beam Yielding

If the frame is designed on the basis of weak-beam strong-column concept, the ultimate strength should be limited by beam flexural. But joint concrete deterioration would occur, because of the shear cracking or bond deterioration by cyclic loading after beam yielding. To avoid shear deterioration in joint prior to ductile frame behavior, the sufficient excess of joint shear strength to beam flexural is needed.

The influence of joint shear deterioration on frame behavior should be considered at first. Test results showed that the damage of joint concrete such as shear cracking and spalling after beam yielding did not make unfavorable effect on strength i.e. ductility, because specimen strength had been kept lager than beam yield strength till large story drift angle of 1/25 in all specimens. There are some possibilities to be considered for that performance.

1) The excess of joint strength estimated by eq.(1) to beam flexural of these specimen were enough large.

2) The amount of joint reinforcement that total yield strength was half of yield force of beam bars was sufficient for confinement of joint core concrete.

Further consideration should be indispensable, and it can be considered that the excess of joint shear strength should be decided by demanded frame ductility.

CONCLUSIONS

Experimental studies on RC interior beam-column subassemblages were carried out using plane and three-dimensional frame specimens. The influence of joint shear input and bond condition of beam bars on frame behavior after beam yielding was examined, in particular about joint concrete deterioration in large displacement.

Following results were derived from two experimental studies.

1) Bond condition of beam bars within joint did not make large influence on energy dissipation of frame, if joint shear deterioration occurred after beam yielding.

2) Joint shear strength was increased by the existence of transverse beams, because they behaved confinement of joint core concrete.

3) The damage of joint core concrete occurred during one way loading up to large displacement made weak in frame performance at following perpendicular loading.

4) If the excess of joint shear strength to beam flexural is enough large, the damage in joint concrete would not make unfavorable effect on frame ductility.

REFERENCES

1.Architectural Institute of Japan (1982), *Standard for Structural Calculation of Reinforced Concrete Structures*
2.Architectural Institute of Japan (1990), *Design Guideline for Earthquake Resistant Reinforced Concrete Buildings Based on Ultimate Strength Concept*
3.Architectural Institute of Japan (1997), *Design Guideline for Earthquake Resistant Reinforced Concrete Buildings Based on Inelastic Displacement Concept (Draft)*